

Nonlinear Optical Properties of chalcogenide thin films

Dr. Arpana Agrawal

Assistant Professor
Dept. of Physics
Shri Neelkantheshwar Government
Post-Graduate College, Khandwa,
Madhya Pradesh, India

Abstract

Nonlinear optical responses of any material are pre-requirement for their applicability for optoelectronic device applications such as optical limiters, saturable absorbers, mode lockers, etc. Such nonlinear optical properties include absorptive/refractive optical nonlinearity, carrier dynamics, etc. For such applications, chalcogenide thin films have proven themselves as potential candidate materials because of their extraordinary nonlinear optical responses. Accordingly, present chapter briefly present an overview of the nonlinear optical properties of various chalcogenide based thin films including transition metal chalcogenide thin films, chalcogenide glasses, chalcogenide/graphene-based thin films, waveguides, quaternary chalcogenides etc.

Experimental findings based on the nonlinear optical properties of chalcogenide-based thin films from several recent studies were accumulated and discussed in detail.

Keywords- Chalcogenide-based thin films, Nonlinear optics, z-scan technique, Nonlinear absorption, Nonlinear refraction

Introduction

Chalcogenides based materials have grabbed tremendous research interest and appear to be a very promising solution for the successful fabrication of optoelectronic devices including mode locker, saturable absorbers, optical limiters, high-performance integrated optical waveguides owing to their several encouraging properties including transparency in visible and infrared (IR) regions, strong light confinement, excellent optical nonlinearity, etc [1]. Possibility of making alloys or glasses utilizing this material adds another dimension to their utility which can be done by alloying chalcogen elements (S, Se, Te etc.) with elements such as As, Sb, Ge, Mo, W, etc. For utilizing such material for optoelectronic device applications, the knowledge of their nonlinear optical (NLO) properties is imperative where the behavior of light as it passes through a nonlinear media is examined under an intense laser light source. Under such a situation, total absorption (α) and total refraction (n) parameters becomes intensity (I) dependent and are given by,

$$\alpha(I) = \alpha_0 + \beta I \dots \dots \dots (i)$$

$$n(I) = n_0 + n_2 I \dots \dots \dots (ii)$$

Here, α_o and n_o are the linear absorption coefficient and linear refractive index, respectively, and β and n_2 are the nonlinear absorption coefficient (NLA) and nonlinear refractive index (NRI), respectively.

To precisely obtain such parameters, z-scan technique based on the principles of spatial beam distortion was developed by Sheikh Bahae et al [2]., and has been employed by various researchers [3-6]. This technique is the simplest and most sensitive experimental tool to determine the magnitude as well as the sign of the NLO whose accuracy depends on how precisely one can determine any variation in the spatial profile of the laser beam. Figure 1 schematically shows the experimental setup for the technique which can be performed in two assemblies: (i) Open aperture (OA) geometry to determine NLA and (ii) Closed aperture (CA) geometry to obtain NLR. In this technique, the sample is mounted on a translation stage to allow its motion in positive and negative z-direction with respect to the focal plane ($z = 0$) of the focusing lens so that intensity variation can be experienced by the sample at different transverse positions. In case of OA geometry, all the transmitted light from the sample is allowed to enter the detector while in case of CA assembly, an aperture is placed in between the sample and the detector so that only an on-axis beam can enter the detector. Absorptive optical nonlinearity may have its origin in saturable absorption (SA) or reverse saturable absorption (RSA) effects which results in negative or positive sign of NLA, respectively,

which can be obtained from theoretical fitting of the experimentally obtained transmittance as a function of transverse distance ($T(z)$) using the equation [7],

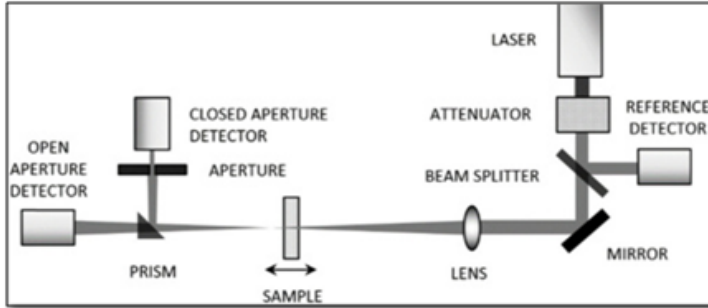


Figure 1. Schematic illustration of z-scan experimental technique under open aperture and closed aperture geometries. (Reproduced from Walden et al. [8]., under a Creative Commons Attribution 4.0 International License)

$$T(z) \approx 1 - \frac{q_o}{2\sqrt{2}\left(1 + \frac{z^2}{z_R^2}\right)} \dots\dots\dots(iii)$$

Here, z_R is the Rayleigh range, q_o is the fitting parameter defined by $q_o = \beta I_o L_{eff}$, with I_o being the maximum intensity at $z = 0$ and L_{eff} is the linear absorption compensated length. In case of SA (RSA), transmittance increases (decreases) with increase in intensity of laser light as sample approaches to focal plane of tight focusing lens and results in various practical applications. Materials with positive NLA have its applicability in optical limiters which are transparent for low input intensities and become opaque for high input intensities after a limiting threshold and hence

protects sensitive components from high intensities. On the other hand, materials with negative NLA are utilized in making saturable absorbers employed in mode locking techniques.

It is worth stressing here that NLR has its origin in either thermal or electronic effects and the sign of NLR depends on the inherent self-focusing or self-defocusing behavior of the material as intense laser light passes through them and consequently, the sample behaves like a lens having variable focal length. The sign of NLR can be obtained by simply visualizing the CA z-scan transmittance signal where pre-focal peak followed by a post-focal valley indicates self-defocusing effect and hence negative refractive optical nonlinearity and vice-versa. Under positive (negative) refractive optical nonlinearity, sample behaves as converging (diverging) lens possessing positive (negative) focal length which tends to converge (diverge) the laser beam upon its propagation through the samples causing self-focusing (self-defocusing) effect.

NLO response of chalcogenide-based nanomaterial thin films is an important decisive parameter for its applicability for specific optoelectronic device applications. Hence it is imperative to examine the optical nonlinearity of such materials. In view of the above discussion, herein an attempt has been made to discuss the NLO properties of various chalcogenide-based nanomaterial thin films along with the results from recent studies.

Nonlinear optical properties of chalcogenide

nanomaterial based thin films

Chalcogenide based nanomaterial thin films including transition metal (TM) chalcogenide (MoS_2 , MoSe_2 , WS_2 , etc) thin films, chalcogenide glasses, chalcogenide/graphene (G)-based thin films, waveguides, quaternary chalcogenides etc., possesses fascinating optical nonlinearity in visible and near IR regime. Kaur et al [9], have studied the linear and NLO properties of MoSe_2 /polymethylmethacrylate (PMMA) composite thin films. Initially, MoSe_2 nanoparticles (NPs) were prepared by hydrothermal method and then the prepared MoSe_2 NPs were mixed with methylmethacrylate (MMA) solution and polymerized to synthesize dispersion of MoSe_2 NPs in PMMA. Finally, MoSe_2 /PMMA composite thin films were deposited by drop casting of glass slides. Absorptive and refractive optical nonlinearity was examined by performing OA and CA z-scan experiment, respectively, using a continuous wave (CW) He-Ne laser ($\lambda = 632.8$ nm). Experimental OA curves exhibit a peak at focal point indicating SA while peak-valley feature was obtained in the CA results suggesting self-defocusing effect and hence the negative sign of NLR. One step chemical vapor deposited (CVD) thin films consisting of mono-/few layer MoS_2 on Si/SiO₂ substrate was also reported to exhibit excellent NLO properties [10]. A CW diode laser was employed to perform z-scan experiment and hence thermal effects are reported to be responsible for the origin of optical nonlinearity in these

chalcogenide thin films. NLO properties of quaternary chalcogenide $\text{Pb}_4\text{Ga}_4\text{GeQ}_{12}$ (Q= S, Se) have been reported by Chen et al [11]. Serna et al [11]., have reported third-order NLO susceptibility of integrated $\text{Ge}_{23}\text{Sb}_7\text{S}_{70}$ chalcogenide glass waveguide in near IR region at a wavelength of 1580 nm using z-scan method. A 420 nm thick layer of $\text{Ge}_{23}\text{Sb}_7\text{S}_{70}$ is evaporated on oxide coated silicon substrate and electron beam lithography and reactive ion etching was employed to define the waveguide. Two-photon absorption with a nonlinear figure of merit of 6.0 ± 1.4 at 1580 nm was obtained.

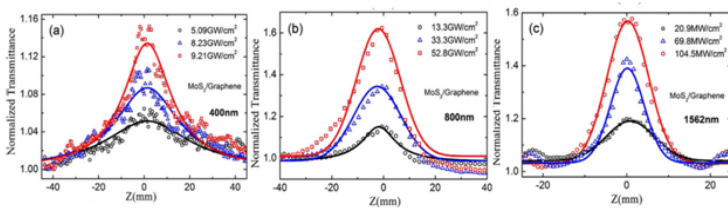


Figure 2. OA z-scan results for $\text{MoS}_2/\text{graphene}$ nanocomposites at 400 nm (a), 800 nm (b) and 1562 nm (c). (Reproduced from Jiang et al. [12]., under a Creative Commons Attribution 4.0 International License)

Jiang et al [12]., have also demonstrated the NLO responses of hydrothermally grown MoS_2/G nanocomposite for ultrafast photonic applications. OA z-scan and pump probe techniques were employed to examine NLO response and carrier dynamics using Ti:Sapphire amplified laser (800 nm). Figure 2(a)-2(c) shows OA z-scan results for MoS_2/G at 400 nm, 800 nm and 1562 nm, respectively, under different input fluencies. Appearance of peak-feature implies SA behavior of

the material with saturation intensity $\sim I_s = 2.44 \text{ mW/cm}^2$ at 1562 nm . Figures 3 illustrates carrier dynamics for MoS_2/G nanocomposite for different pump intensities, which clearly shows pump-power intensity independent relaxation-time with fast and slower relaxation time constants $1.3 \pm 0.2 \text{ ps}$ and $36 \pm 2 \text{ ps}$ at a power of 0.354 GW/cm^2 , respectively.

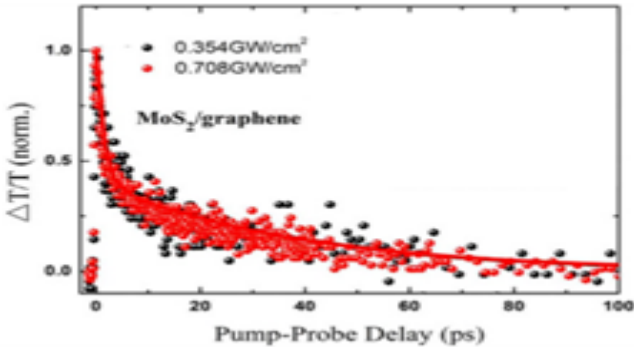


Figure 3. Carrier dynamics of $\text{MoS}_2/\text{graphene}$ nanocomposite under different pump power intensities. (Reproduced from Jiang et al. [12]., under a Creative Commons Attribution 4.0 International License)

Enhanced optical nonlinearity in G/MoS_2 organic glasses as compared to MoS_2/PMMA (365 cm/GW) has been reported by Ouyang et al [13]. Initially, G/MoS_2 composite was hydrothermally prepared and then dispersed in MMA followed by polymerization to finally prepare G/MoS_2 organic glass. NLA response was examined by performing OA z-scan experiment and a dip-like feature was experiential in the transmittance signal signifying the positive sign of NLA with magnitude of $\sim 2110 \text{ cm/GW}$ and the occurrence of RSA and hence indicates the applicability for optical limiting applications.

Tunable NLA in WS_2 /PMMA composite have been demonstrated by Long et al [14]., where WS_2 nanosheets (NSs) were initially synthesized by ultrasonication assisted liquid phase exfoliation and then dispersed in MMA followed by heat treatment at certain temperature and time. Finally, solid transparent WS_2 /PMMA composite were obtained which were examined via OA z-scan employing a pulsed Nd:YAG laser. Rahmati et al [15]., have illustrated the NLO properties of CVD grown vertically aligned MoS_2 NSs on quartz substrate where a dip-like feature in OA geometry and valley-peak feature in CA geometry was observed signifying RSA and self-focusing effect of MoS_2 /quartz, respectively. **Table 1** summarizes few experimentally obtained NLO parameters for chalcogenide nanomaterial based thin films.

Table 1. Experimentally obtained NLO parameters for chalcogenide nanomaterial based thin films.

Material	Laser parameter	NLO properties	Ref.
$Ge_{23}Sb_7S_{70}$	1580 nm	NLA = 0.010 ± 0.03 cm/GW NLR = $0.93 \pm 0.08 \times 10^{-18}$ m ² /W	[1]
$MoSe_2$ / PMMA	632.8 nm; 3.93×10^3 W/m ²	NLA – 4.68×10^{-8} cm/W NLR = -6.76×10^{-7} cm ² /W	[9]

MoS ₂ (150 nm)/SiO ₂ /Si	532 nm	NLA = 63.07 cm/W NLR = -2.3×10^{-3} cm ² /W	[10]
MoS ₂ (230 nm)/SiO ₂ /Si	532 nm	NLA = 72.85 cm/W NLR = -0.9×10^{-3} cm ² /W	[10]
MoS ₂ (420 nm)/SiO ₂ /Si	532 nm	NLA = 80.53 cm/W NLR = -3.9×10^{-3} cm ² /W	[10]
G/MoS ₂ /PMMA	532 nm; 6 ns; 1Hz; 66 μJ	NLA = 2110 cm/GW	[13]
WS ₂ /PMMA	1064 nm; 8 ns; 10 Hz	NLA = 21.87 cm/GW	[14]
MoS ₂ /quartz	532 nm	NLA ≈ 1 cm/W NLR ≈ 10^{-5} cm ² /W	[15]
MoSe ₂ /G	532 nm; 30 ps; 10 Hz; 6.6 GW/cm ²	NLA = -3.90×10^{-12} m/W NLR = 1.18×10^{-11} esu	[16]
MoS ₂ /G	800 nm; 1 Hz	NLA ~ -1217.8 cm/GW	[17]

Conclusion

To conclude, this chapter briefly describes the NLO properties of various chalcogenide-based nanomaterial thin films including TM chalcogenide thin films, TM chalcogenide/graphene(G)-based thin films, chalcogenide glasses, waveguides, quaternary chalcogenides, etc. Outcomes from various recent studies have been compiled and presented which can serve as a guide for users to search the specific chalcogenide material data and possibly utilize it for fabricating optoelectronic devices. Overall, it can be evident from the discussions present in the chapter that chalcogenide thin films grab phenomenal potential as an optoelectronic material, owing to its excellent nonlinear optical properties.

References

1. Serna, Samuel, et al. "Nonlinear optical properties of integrated GeSbS chalcogenide waveguides." *Photonics Research* 6.5 (2018): B37-B42.
2. Sheik-Bahae, et al. "High-sensitivity, single-beam n_2 measurements." *Optics Letters* 14.17 (1989): 955-957.
3. Agrawal, Arpana, et al. "Insight into the effect of screw dislocations and oxygen vacancy defects on the optical nonlinear refraction response in chemically grown ZnO/Al₂O₃ films." *Journal of Applied Physics* 122.19 (2017): 195303.
4. Agrawal, Arpana, et al. "Unraveling absorptive and refractive optical nonlinearities in CVD grown graphene

-
- layers transferred onto a foreign quartz substrate." Applied Surface Science 505 (2020): 144392.*
5. Agrawal, Arpana, et al. "Study of nonlinear optical properties of pure and Mg-doped ZnO films." *Physica Status Solidi (b) 252.8 (2015): 1848-1853.*
 6. Dar, Tanveer Ahmad, et al. "Thermo-optic coefficients of pure and Ni doped ZnO thin films." *Thin Solid Films 603 (2016): 115-118.*
 7. Agrawal, Arpana, et al. "Negative thermo-optic coefficients and optical limiting response in pulsed laser deposited Mg-doped ZnO thin films." *Journal of Optical Society of America B 33.9 (2016): 2015-2019.*
 8. Walden, Sarah L., et al. "Accurate determination of nonlinear refraction in ZnO and Au composite nanostructures." *Optical Materials Express 10.2 (2020): 653-661.*
 9. Kaur, Ravneet, et al. "Study of linear and non-linear optical responses of MoSe₂-PMMA nanocomposites." *Journal of Materials Science: Materials in Electronics 31.22 (2020): 19974-19988.*
 10. Mirershadi, Soghra, et al. "Non-linear thermo-optical properties of MoS₂ nanoflakes by means of the Z-scan technique." *Frontiers in Physics 8 (2020): 96.*
 11. Chen, Yu-Kun, et al. "Syntheses, structures, and nonlinear optical properties of quaternary chalcogenides: Pb₄Ga₄GeQ₁₂ (Q= S, Se)." *Inorganic Chemistry 52.15 (2013): 8334-8341.*

12. Jiang, Yaqin, et al. "Broadband and enhanced nonlinear optical response of MoS₂/graphene nanocomposites for ultrafast photonics applications." *Scientific Reports* 5.1 (2015): 1-12.
13. Ouyang, Qiuyun, et al. "Graphene/MoS₂ organic glasses: Fabrication and enhanced reverse saturable absorption properties." *Optical Materials* 35.12 (2013): 2352-2356.
14. Long, Hui, et al. "Tuning nonlinear optical absorption properties of WS₂ nanosheets." *Nanoscale* 7.42 (2015): 17771-17777.
15. Rahmati, Bahareh, et al. "Nonlinear Optical Properties of Vertically-Aligned MoS₂ Nanosheets." *Journal of Electronic Materials* 50.6 (2021): 3645-3651.
16. Liu, Gangshuo, et al. "Third-order nonlinear optical properties of MoSe₂/graphene composite materials." *Optics & Laser Technology* 120 (2019): 105746.
17. He, Minmin, et al. "Enhanced nonlinear saturable absorption of MoS₂/graphene nanocomposite films." *The Journal of Physical Chemistry C* 121.48 (2017): 27147-27153.